Reviews

Oncogene mRNA imaging with ^{99m}Tc-chelator-PNA-peptides

E. Wickstrom,[a,b]★ X. Tian,[a,b] P. S. Rao,[b,c] M. L. Thakur,[b,c] W. Qin,[b,d] and E. R. Sauter[b,d]

Departments of [a]Microbiology and Immunology, [b]Radiology, [c]Surgery, and [d]Kimmel Cancer Center, Thomas Jefferson University, 19107 Philadelphia PA, USA.
Fax: +1 (215) 955 4580. E-mail: eric@tesla.jci.tju.edu

[^{99m}Tc]PNA-peptide conjugates capable of binding to IGF1 receptors will be synthesized. Specificity of their uptake and hybridization to mRNA in normal epithelial human cells compared to human breast cancer cells will be studied.

Key words: cancer, imaging, oligonucleotides, oncogenes, peptides, radionuclides, receptors.

Problem anakysis

No method is currently available to measure levels of specific mRNAs non-invasively in living cells and tissues. As a diagnostic tool for measuring gene expression, peptide nucleic acids (PNAs) display superior ruggedness and hybridization properties. However, they are negligibly internalized by normal or malignant cells. We have previously observed that ^{99m}Tc-peptides can delineate tumors, that ^{99m}Tc-chelator-DNA-peptides can be synthesized, that PNA-peptides are specific for receptors on malignant cells, and that PNA-peptides are taken up specifically and concentrated in nuclei of malignant cells. Therefore we hypothesize that antisense ^{99m}Tc-chelator-PNA-peptides will be taken up by human cancer cells, hybridize to complementary mRNA targets, and permit imaging of hybridized oncogene mRNAs in human cancer xenografts in a mouse model. The oncogenes cyclin D1, *ERBB*2, c-*MYC*, and tumor suppressor p53 will be probed. These experiments will test our concept for noninvasive detection of gene expression in living cells and tissues. Such a scintigraphic imaging technique should be applicable to any particular gene of interest in a cell or tissue type with characteristic receptors.

1.1. Cancer diagnosis *via* gene expression. The ultimate pathology of all proliferative diseases results from molecular genetic modulations at a cellular level, induced by activation of oncogenes. A broad spectrum of genes associated with many types of malignancies has been identified. Imaging gene expression, non-invasively, with high sensitivity and specificity, can become a more powerful diagnostic tool than any currently available. While non-invasive positron emission tomography (PET) with [^{18}F]-fluoroguanine derivatives[1] may in the future permit imaging of sites of cellular proliferation, it will not provide the identities of overexpressed genes. PET measurement of tumor uptake of an [^{18}F]-fluoroguanine derivative that is specifically phosphorylated by herpes simplex virus thymidine kinase (HSVTK) represents the

Published in Russian in *Izvestiya Akademii Nauk. Seriya Khimicheskaya,* No. 7, pp. 997—1013, July, 2002.

1066-5285/02/5107-1083 $27.00

closest approach so far to determination of specific gene expression, in a case where the tumors were directly transformed by adenoviral vectors carrying HSVTK.[2] Similarly, PET measurement of tumor uptake of [^{18}F]-2′-deoxy-2′-fluoro-5-iodouridine arabinoside (FIAU) in tumor cells retrovirally transformed with HSVTK expressed from a p53-controlled promoter indirectly implied elevated expression of p53.[3] In contrast to the indirect [^{18}F] approaches, we hypothesize that non-invasive administration of ^{99m}Tc-PNA-peptides specific for particular oncogene mRNAs will allow us to image pre-cancerous cells overexpressing each specific oncogene. In view of the frustrating difficulties for unambiguous early diagnosis of breast cancer, we propose to use human breast cancer cells grown in athymic nude mice as our first model system.

1.2. Breast cancer diagnosis. In 2001, invasive breast cancer will attack approximately 190,000 US women, and this malignancy will take the lives of approximately 41 000 patients.[4] Breast cancer is the leading cause of cancer in US women (excluding skin cancers). In men, about 1400 new breast cancers will present in 2001. Breast cancer incidence rates for women have increased 2% per year since 1980. Currently, 110 breast cancers occur every year per 100 000 women. The 5-year survival rate is 94% if the disease is localized to the breast, 73% if the disease has spread regionally, but only 18% for patients with distant metastases at the time of diagnosis. Mortality rates for mammary cancer remain high, despite recent advances in the treatment of advanced disease, screening for early cancer, and fundamental knowledge about the molecular and cellular events that underlie this disease.

Mammography and physical examination, the only generally accepted screening tools available, miss up to 40% of early breast cancers. Moreover, if an abnormality is found, an invasive diagnostic procedure must still be performed to determine if the breast contains atypia or cancer, even though 85% of abnormalities are benign.[5] Present diagnostic techniques include needle biopsy, excisional biopsy, and mastectomy. Each procedure has the risk of hematoma formation and infection. The first procedure is limited by sampling error, while the latter two require costly operative procedures and raise concerns regarding cosmesis.

Diagnostic efforts to identify women with precancerous changes or breast cancer are hindered by the fact that the evaluation of the breast has traditionally required a surgical biopsy. A non-operative method to evaluate women for the presence of atypia and cancer of the breast, whether performed as routine screening or to evaluate an abnormality found on breast exam or mammogram, would be very beneficial.

1.3. Oncogenes associated with breast cancer. Cancerous cells display overexpression or mutant expression of one or more of the 5000 genes normally used in cell proliferation.[6] Such genes are called proto-oncogenes.[7] The implication is that the targets that must be attacked in breast tumor cells are normal cellular genes that have sustained some activating lesion. Cyclin D1, *ERBB2*, and c-*MYC* oncogenes, as well as the tumor suppressor p53, are frequently overexpressed in breast cancer cells. Oncogene-targeted antisense DNA sequences specifically down-regulate cyclin D1,[8] *ERBB2*,[9,10] c-*MYC*,[11–14] and p53,[15,16] inhibiting cancer cell proliferation. Thus we hypothesize that those mRNAs are significant markers of oncogenic transformation that we may utilize to distinguish cancerous masses from benign cysts in breasts. Microarray analyses of mRNA expression patterns in breast cancer cells have not yet identified detectable overexpression of those markers,[6] and that approach could only be applied to invasive biopsy tissue.

1.3.1. Cyclin D1. Cyclin D1 (BCL1, PRAD1, CCND1) is a proto-oncogenic regulator[17] of the G1/S checkpoint in the cell cycle that has been implicated in the pathogenesis of several types of cancer, including breast cancer. The cyclin D1 protein is overexpressed in up to 80% of tumors.[18,19] There is substantial evidence that critical regulatory steps occur during the cell cycle that determine whether or not the cell will synthesize new DNA and divide. These critical regulators of G1 are frequent targets for mutations.[20] Among the most frequently mutated genes are those that control the checkpoint (often called the restriction or R point) in late G1. The major regulator of this checkpoint appears to be pRb, the protein product of the retinoblastoma gene.[21] When hypophosphorylated, pRb inhibits cell growth by binding to, and preventing the function of, a number of transcription factors, including some in the E2F family.[20] Phosphorylation of pRb in mid to late G1 releases the transcription factor(s) bound by pRb that leads to DNA synthesis.[22] Two important regulators of G1 are p53 and cyclin D1. p53 appears to suppress cell division by stimulating the synthesis of a cyclin-dependent kinase (Cdk) inhibitor, p21.[23] Cyclin D1 appears to function upstream of pRb by binding to cyclin-dependent kinase (cdk) 4 or 6, leading to pRb phosphorylation by the cdk.[24]

Amplification is only one method by which the protein product can be overexpressed. Increased expression has also been observed due to gene rearrangement[25,26] both in parathyroid tumors (11q13 with 11p15) and B cell tumors (11q13 with 14q32). Overexpression of cyclin D1 in cultured cells leads to a more rapid transversion through the G1 phase of the cell cycle and entry into S phase.[27,28] Cyclin D1 cooperates with Ras protein[17] and complements a defective E1a adenoviral gene[29] to function as an oncogene.

Cyclin D1 levels decrease with melanoma differentiation,[30] and neutralizing antibodies to cyclin D1 ar-

rested the melanoma cell line SK29-MEL-1 in G1 whereas p16 did not, suggesting that cyclin D1 plays an important and perhaps essential role in melanoma growth and progression. Indeed we observed that cyclin D1 antisense DNA sequences specifically down-regulate cyclin D1, and inhibit proliferation, in melanoma cells.[8]

Cyclin D1 overexpression and amplification is an early event in breast carcinogenesis, being found in up to 30% of *in situ* lesions.[31] Fully half of invasive breast cancers have increased cyclin D1 protein expression.[32] In view of the observation that cyclin D1 expression is associated with poor prognosis in breast cancers,[33,34] and our ability to suppress cyclin D1 expression with antisense RNA vectors,[35] it is reasonable to hypothesize that cyclin D1 antisense oligonucleotides labeled with ^{99m}Tc could identify malignant atypia detected by mammography, or pre-malignant zones that were not detected by mammography.

1.3.2. *ERBB*2. Amplification of the *ERBB2* gene was first identified as a marker of advanced stage breast cancer and a prognostic marker.[36] Subsequent studies demonstrated the overexpression and amplification of *ERBB2* gene in carcinomas *in situ*.[37] A recent study demonstrated low-level (two- to four-fold) *ERBB2* gene amplification in 9.5% of benign breast tissue specimens in which adjacent tumor was present.[38] The presence of proliferative cytology and *ERBB2* amplification implied an odds ratio of 7.2 for the future development of breast cancer, compared to biopsies lacking breast proliferation and *ERBB2* amplification.[38]

ERBB2 gene encodes a 185 kDa protein, ErbB2, belonging to the receptor-tyrosine kinase family of cell surface proteins.[39] The ErbB2 protein displays strong homology with epidermal growth factor receptor,[40] as do the closely related ErbB3 and ErbB4 receptors.[41,42] All three receptors are located on epithelial cell surfaces in sufficient proximity that they may be crosslinked. The activation of the intracellular tyrosine kinase activity is most likely the key step by which p185 confers transforming signals to second messenger systems, such as the Ras pathways. ErbB2 receptor does not appear to be expressed in normal adult cells, except for secretory epithelial cells, and may only be generally necessary at an early developmental stage.[43] While ErbB2 overexpression is associated with poor prognosis, this receptor may not be the key to malignant cell proliferation, but rather to recurrence, a more formidable problem.[44]

There is significant evidence that ErbB2 status is helpful in predicting response to therapy, whether hormonal, cytotoxic, or radiation.[45] Serum-based testing for circulating ErbB2 protein also shows promise, as most though not all studies suggest that elevated levels of ErbB2 in serum correlate with decreased survival and absence of clinical response to hormone therapy.[45] A humanized monoclonal antibody to ErbB2, Herceptin^{R}, has a favorable toxicity profile and has efficacy in ErbB2 positive metastatic breast cancer both alone[46] and in combination with chemotherapy.[47]

While tissue-based detection of ErbB2 remains the clinical standard, there is disagreement as to the best method of measuring overexpression.[45] For comparative purposes, we have chosen to detect *ERBB2* amplification through a highly sensitive PCR technique and ErbB2 overexpression by immunostaining, which allows us to evaluate the tissue *in situ*. One advantage of PCR is that it can detect low-level amplification in histologically benign tissue adjacent to breast cancer, whereas overexpression is not seen in this setting. Women with histologically benign but *ERBB2* gene-positive tissue appear to be at increased breast cancer risk.[38]

Antisense DNA has been applied against *ERBB2* and was observed to decrease p185 levels.[9,48,49] This has prevented tumorigenesis by *ERBB2*-transformed SKOV3 ovarian carcinoma cells in immunocompromised mice.[10,50] Hence, *ERBB2* mRNA appears to be another logical target for antisense ^{99m}Tc detection of oncogene expression in breast cancer.

1.3.3. Proto-oncogene c-*MYC*. The proto-oncogene c-*MYC* is amplified and/or overexpressed in about 30% of both advanced and early stage mammary tumors.[51] The target oncogene, c-*MYC*, expresses a nuclear protein Myc with an electrophoretic apparent molecular mass of 65 kDa (p65). Myc is one of the leucine zipper proteins, which binds with a small partner protein, Max, and this heterodimer in turn binds specifically to the sequence dGACCACGTGGTC which occurs in the regulatory regions upstream of proliferative genes.[52] Expression of the c-*MYC* gene is normally controlled by a variety of transcriptional activating proteins[53] and suppressor proteins such as p53.[54]

c-*MYC* was the first oncogene targeted by antisense DNA, specifically the MYC6 sequence,[11] and a number of c-*MYC* antisense sequences have displayed sequence-specific antisense activity in a variety of malignant cells in culture[55] and in animal hosts.[56] In breast cancer, the c-*MYC* antisense sequence MYC6 displayed gene inhibition and antiproliferation activity in estrogen-stimulated MCF7 cells[57] and in SKBR3 cells (see below). These results provide a reasonable basis for pursuing c-*MYC* mRNA as a logical target for probing with antisense ^{99m}Tc in breast atypia.

1.3.4. p53. Mutations in the p53 tumor suppressor gene are common in breast cancer, with frequencies of 20—61% being observed.[58] There is a high association between p53 mutations and p53 protein accumulation,[59] such that many researchers now accept p53 overexpression as a valid surrogate for p53 mutations.[60] One large study[59] observed p53 overexpression in 16% of *in situ* carcinomas, 22% of sporadic carcinomas, 34% of tumors from patients with familial breast cancer, and 52% of tumors

from patients with familial breast and ovarian cancer syndrome.

Targeted therapy of human cancer based on molecular alterations in p53 are being studied in both preclinical and clinical settings. Adenoviral mediated transfection of immortalized Li-Fraumeni cells increased the efficacy of photodynamic therapy in inducing apoptosis.[61] Adenovirus-mediated p53 gene therapy has been shown to enhance chemotherapy in preclinical models of human cancer[62] and is currently being conducted in clinical trials with low toxicity and evidence of antitumor activity.[63] p53 overexpression leads to enhanced radiosensitivity of tumors, both after adenoviral transduction[64] and with a liposome-mediated vehicle for delivery of therapy.[65]

Oncogene-targeted antisense DNA phosphorothioate sequences have been observed to down-regulate p53 specifically in malignant hematopoietic cells,[15,16] inhibiting leukemic cell proliferation.[15,16] Hence, p53 mRNA appears to be another logical target for antisense ^{99m}Tc detection of oncogene expression in breast cancer.

1.4. Antisense oligonucleotide derivatives. The ability to turn off individual genes at will in growing cells provides a powerful tool for elucidating the role of a particular gene for diagnosis and for therapeutic intervention. Antisense DNAs (Fig. 1) were first conceived as alkylating complementary oligodeoxynucleotides directed against naturally occurring nucleic acids[66] and first successfully utilized against Rous sarcoma virus.[67] Since those proofs of principle, antisense DNA derivatives have been utilized to inhibit the expression of a wide variety of target genes in viral, bacterial, plant, and animal systems, in cells,[55] in animals,[68] and in humans.[69] Backbone modifications of antisense DNAs (Fig. 2) have been found to increase lifetime and efficiency. Despite their efficacy, however, phosphorothioate DNAs exhibit less sequence specificity in their effects than do phosphodiesters or methylphosphonates,[55,70] due to significant binding to a spectrum of plasma and cellular proteins.[71] Encouraging results have been obtained recently suggesting that greater potency and specificity might be possible with 2´-O-alkyl RNA/DNA/2´-*O*-alkyl RNA phosphorothioate chimeras,[72,73] PNA-peptide conjugates,[74] $\alpha/\beta/\alpha$-anomeric DNA chimeras,[75,76] DNA boranophosphates,[77,78] or peptide-DNA conjugates.[79,80]

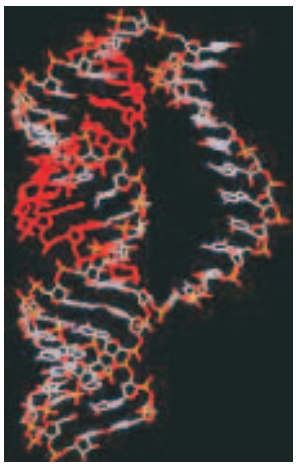

Fig. 1. Antisense DNA (red) basepaired to mRNA target.

Antisense DNA therapeutics have already overcome several hurdles. These include uptake by cells, survival in cells, reaching target mRNA in cells, blocking gene function with predicted specificity, displaying significant anti-cancer or anti-viral effects as a result of gene blockage, nontoxicity in mice, and efficacy in mice. Over a dozen clinical trials are underway for a number of indications, using phosphorothioates.[69] In 1998, FDA issued its first approval of a therapeutic oligonucleotide targeted against cytomegalovirus.[81] Antisense diagnostics have not advanced comparably, at least in part because charged antisense DNAs hybridized to RNA form a substrate for RNase H,[82] leading to the destruction of the message that one might wish to measure. On this campus, we looked for accumulation of labeled *ERBB2* antisense oligonucleotide phosphorothioate, compared with a scrambled control, in SKBR3 cells that overexpress *ERBB2* mRNA, but found equivalent amounts of label in each cellular preparation.* Similarly, a ^{99m}Tc-labeled HYNIC-conjugated oligonucleotide *ERBB2* antisense oligonucleotide phosphorothioate did not show differences in uptake among cell lines with high, normal, or low levels of c-*MYC* mRNA.[83] We think, however, that peptide nucleic acids (PNAs) (Fig. 2) will overcome the problems of charged DNA as antisense diagnostic probes.

1.5. Imaging with ^{99m}Tc-ligands. For imaging gene expression we prefer to use ^{99m}Tc because of its universal availability from ^{99}Mo generator and its physical decay characteristics. It has a half-life of six hours, which is long enough to permit imaging gene but not too long to persist in the body and impart unnecessary radiation dose to the patient. It also decays with emission 140 keV gamma rays (90%) that can be efficiently detected externally by a commonly available device, the gamma camera. Currently nearly 90% of all scintigraphic imaging procedures use ^{99m}Tc.

The use of other positron emitting radionuclides such as [^{18}F] is becoming increasingly popular for scintigraphic imaging by PET scanners or coincidence gamma cameras. However, [^{18}F] requires a cyclotron to produce, has a half-life of only 110 min, and it is not yet commercially available in the fluoride form essential for synthesis of [^{18}F]PNAs. Furthermore, imaging lesions requires an expensive PET scanner or coincidence cameras, avail-

* Basu, Wickstrom, and Thakur, unpublished results.

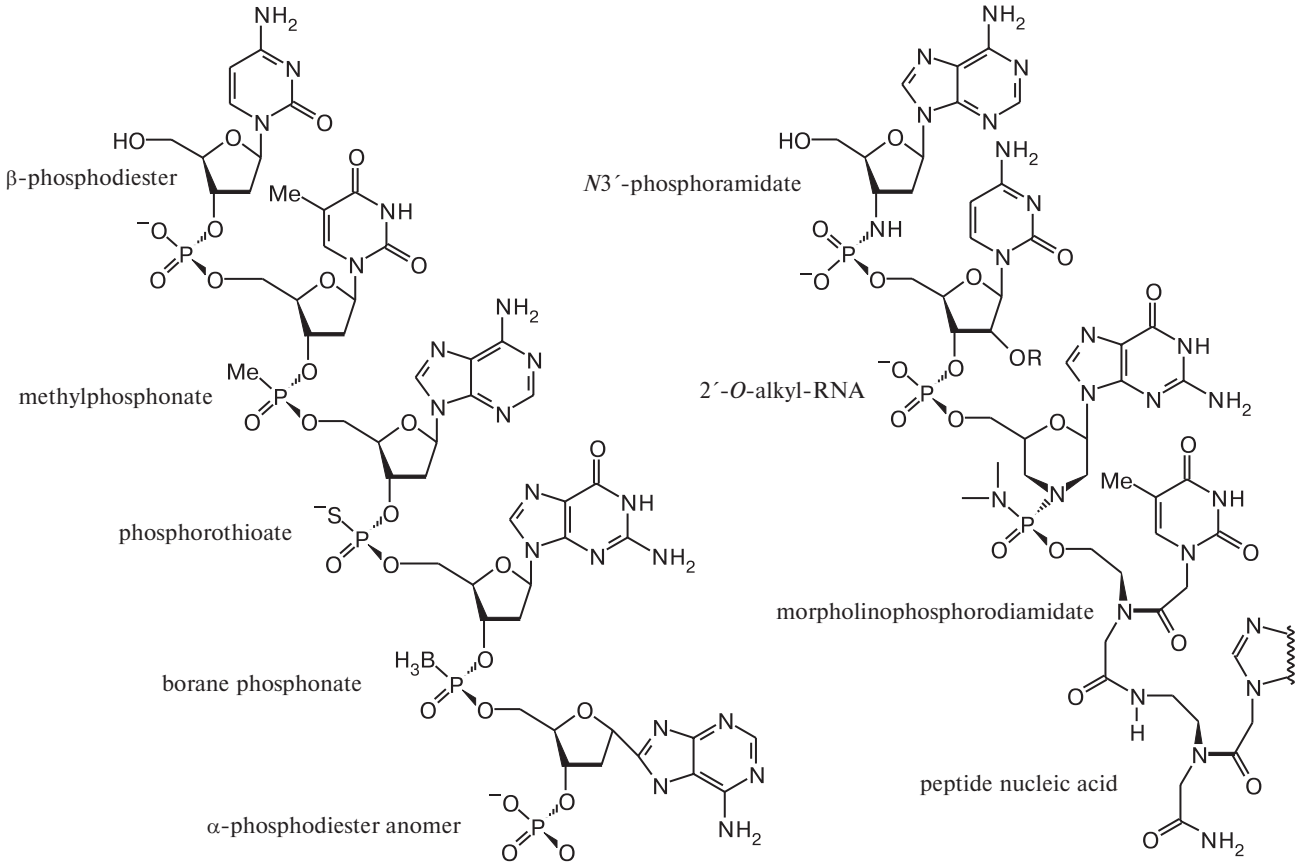

Fig. 2. Oligonucleotide backbone derivatives.

able at present in less than 2% of the nation's estimated 5000 nuclear medicine centers.

2. Results of studying conjugates

2.1. ^{99m}Tc-peptide imaging. We have developed facile methods for labeling peptides with ^{99m}Tc,[84,85] which also work well with PNA-peptides.* The tetrapeptide Gly—D-Ala—Gly—Gly (GAGG) (Fig. 3, *A*) chelates ^{99m}Tc firmly and efficiently.[84,85] The peptide NH groups of GAGG provide an N_4 configuration for strong chelation of ^{99m}Tc. Not only is the labeling efficiency high (>95%), but also the tracer is stable *in vivo*, even in acidic vesicles. The Gly_4 spacer on the N-terminus of the PNA (Fig. 3, center) is not likely to bind ^{99m}Tc significantly. Using a spacer such as 4-aminobutyric acid (Aba) between the primary peptide and GAGG minimizes steric hindrance from the chelating moiety and the ^{99m}Tc chelate. This technique can also be used to label PNAs with rhenium radionuclides (*e.g.*, ^{186}Re and ^{188}Re) of therapeutic importance. More importantly, the GAGG—Aba chelating sequence can be included with a PNA-peptide during solid phase synthesis, thereby eliminating the need for post-synthetic conjugation (GAGG—Aba—PNA-peptide), purification, and characterization of the required compound (GAGG—Aba—PNA-peptide) (See Fig. 3).

Using this technique, several peptides, such as vasoactive intestinal peptide (VIP) have been labeled with ^{99m}Tc in the Thakur laboratory and successfully evaluated *in vitro*, in experimental animals, and in humans.[84—86] Similar success was obtained upon ^{99m}Tc labeling of the chemotactic peptide fMet—Leu—Phe to image sites of infection.[87] [^{123}I]VIP has already been utilized for imaging pancreatic cancer sites.[88] The Eisenhut group has also prepared and tested the cellular binding of *BCL2* antisense phosphorothioate[89] and PNA[90] sequences conjugated to [^{125}I]Tyr(3)-octreotate.

2.1.1. Preparation of ^{99m}Tc-peptides. The most common way to label peptides with radionuclides has been to synthesize a required peptide and then to conjugate it to a chelating agent that will form a complex radioactive metal ion and facilitate radiolabeling. In this process, however, the peptide functional groups must be protected so that the peptide can neither lose its active groups nor can the chelating agent bind to other peptide side chains but only to the intended terminal groups. Additionally, at the end of the conjugation process the

* Unpublished results.

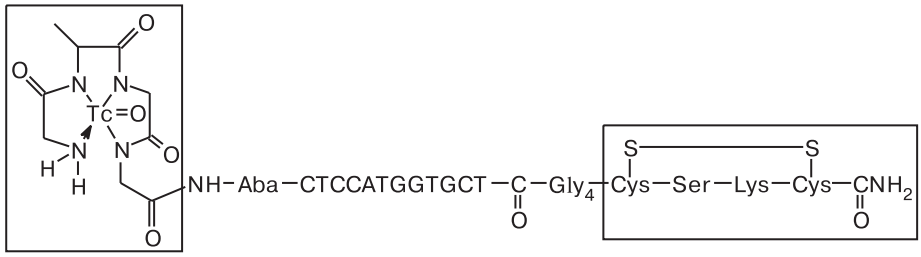

Fig. 3. ^{99m}Tc-chelate-PNA-peptide example.

pre-protected peptide groups must be deprotected and the final product must be purified and characterized. This process is time-consuming and subject to poor yields.

We use Gly—D-Ala—Gly—Gly (GAGG) as a chelating moiety, permitting us to synthesize a peptide of a given sequence with a chelating moiety as its integral part. The entire sequence can be synthesized, purified, and characterized in one process yielding an end product ready to be labeled with ^{99m}Tc. Between the primary peptide and the GAGG we have inserted 4-aminobutyric acid (Aba) as a spacer that eliminates or minimizes the steric hindrance. We now use this technique to synthesize our PNA probes with Aba as a spacer and GAGG as a chelating moiety on the N-terminus of the chosen PNA. Using this process, we can label PNAs without an excessive loss of time or effort. As can be seen below, this labeling procedure does not lead to the loss of biological activity or receptor specificity.*

2.1.2. ^{99m}Tc-peptide binding to cells. Each labeled peptide, VIP—Aba—GGAG—^{99m}Tc (TP3654), ^{99m}Tc—CPTA—VIP, and [^{125}I]VIP, can be evaluated for receptor specificity using a receptor displacement assay, cell binding assays, and muscle relaxivity.[91] Scatchard plot binding analyses (Fig. 5) were performed on HT29 colorectal cancer cells, yielding IC50 values for [^{125}I]VIP displacement of 15 *nM* for both unmodified VIP and for VIP-chelator (TP3654). Measurements of muscle relaxivity in opossum anal smooth muscle strips illustrated similar activity by unmodified VIP and VIP-chelator (TP3654), but reduced activity by CPTA-VIP (Fig. 6). Hence, the biological activity and receptor specificity of VIP were not altered by the Aba-GGAG chelator peptide.[91]

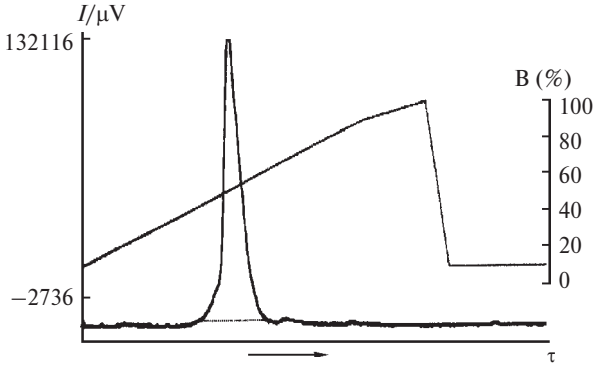

Fig. 4. Analytical HPLC of VIP-chelator-^{99m}Tc (TP3654) on C_{18} column eluted with a gradient from 0.1% CF_3CO_2H in water (system A) to 0.1% CF_3CO_2H in acetonitrile (system B). *I* is γ-radiation intensity.

2.1.3. ^{99m}Tc-peptide imaging of murine tumors. The purpose of this examination was to study the stability of

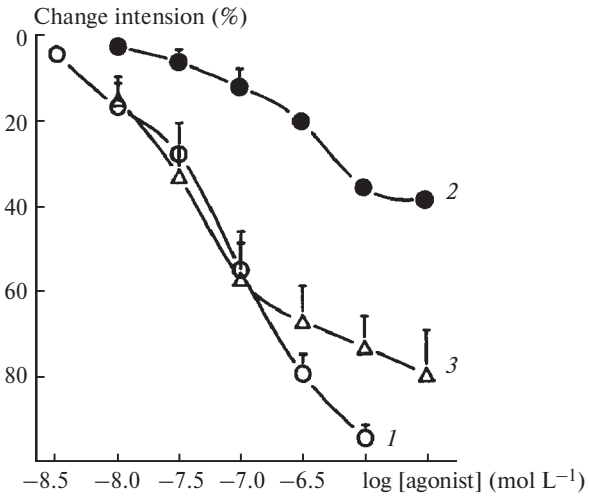

Fig. 5. Internal anal sphincter muscle tension as a function of VIP-chelator (TP3654) (*1*), CPTA-VIP (*2*), or unmodified VIP (*3*).

* As a general rule, 10 μg of each Aba—GAGG modified peptide was added to 650 μL of 0.05 Na_3PO_4, pH 12, 75—100 μg of $SnCl_2$ at 10 g L^{-1} in 0.05 *M* HCl, and the required quantity of ^{99m}Tc in 200 μL of 0.15 *M* NaCl, followed by incubation for 15 min at 90 °C. The reaction mixture was cooled to 22 °C and 1 mL of 0.05 *M* NaH_2PO_4, pH 4.6, was added to bring the pH of the reaction mixture to pH 7.0—7.2. Labeled peptides were analyzed by C_{18} reversed phase HPLC using gradient solvent consisting of 0.1% trifluoroacetic acid in H_2O (solvent A) and 0.1% trifluoroacetic acid in acetonitrile (solvent B). The actual gradient was varied from peptide to peptide so that a good separation between free ^{99m}Tc, if any, and bound ^{99m}Tc could be obtained. The HPLC is equipped with a variable range UV detector and a NaI (Tl) radioactivity monitor. In all peptides, generally unbound ^{99m}Tc was <5% and bound ^{99m}Tc was eluted as a single peak indicating the absence of isomers (Fig. 4).[84,85,91,92]

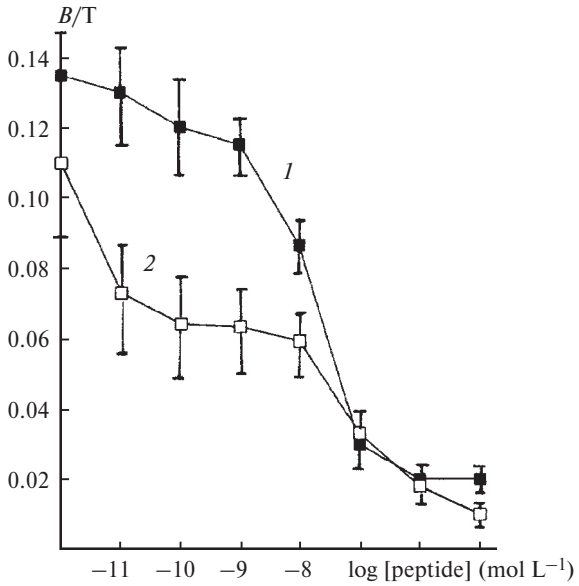

Fig. 6. Scatchard plot of 40 pM [^{125}I]VIP displacement from HT29 colorectal cancer cells by VIP-chelator (TP3654) (*1*) and unmodified VIP (*2*).

the tracer *in vivo*, to determine its metabolites excreted in urine, to assess its blood clearance, to characterize its pharmacokinetics and tissue distribution, and to evaluate its ability to target the intended *in vivo* abnormalities. Studies were performed in mice, rabbits, or pigs.[84,85,87,91,92] In each species, experimental lesions were induced by a suitable experimental procedure approved by the Institutional Animal Care and Use Committee. Peptides intended for detection of venous thrombosis and pulmonary embolism were studied in rabbits and pigs and those for imaging abscesses and tumors were evaluated in mice. Human tumors were grown in nude mice by implanting tumor cell lines maintained in tissue culture. Receptor blocking assays were performed to demonstrate that the uptake in the lesion was receptor specific. Results were generally compared with those of ^{125}I-labeled primary peptides. In all cases, tumors were delineated with high signal/background ratios.[84,91,92] Figure 7 provides an example of a gamma camera image of a mouse bearing experimental human colorectal cancer.[91] The mouse was injected with approximately 700 μCi ^{99m}Tc-VIP or ^{99m}Tc-chelator 24 h previously. The tumor in the right flank was unequivocally delineated by ^{99m}Tc-VIP. In mice in which 50 μg of VIP was injected to preblock the receptors on the tumor cell surfaces, significantly ($p < 0.05$) less ^{99m}Tc-VIP radioactivity was taken up by the tumor.

2.1.4. Imaging tumors in humans with ^{99m}Tc-peptides. Encouraged by the preclinical evaluation results, we initiated a feasibility study of using ^{99m}Tc-VIP for imaging tumors in humans. All tumors as identified by CT, MRI, ^{99m}Tc-SestaMIBI, sonography, or mammography were

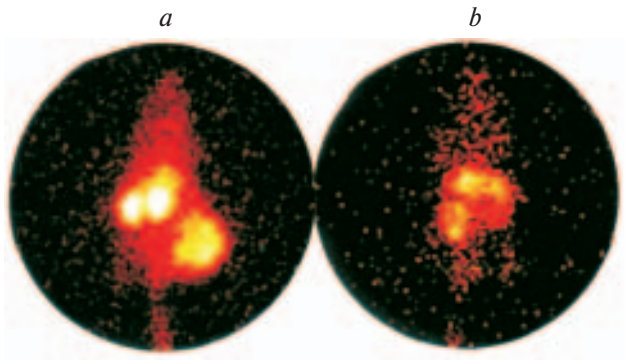

Fig. 7. Posterior gamma camera images of nude mice bearing LS174T (~1 g) human colorectal tumor in right thigh 24 h after injection of VIP-chelator-^{99m}Tc (left) or just chelator-^{99m}Tc control (right). Despite marginal uptake (0.2% I.D./g), tumor in right thigh was delineated (average of 8 pulses) with ^{99m}Tc-VIP because of low body background. This tumor was not delineated with ^{99m}Tc-G(D)AGG-Aba (right).

known to express VIP receptors (VPAC1, VPAC2) in high density.[93] Negative controls did not display inappropriate concentration of labeled VIP (Fig. 8). Out of 11 patients examined thus far, there was concordance in nine patients. In the other two patients, only ^{99}Tc-VIP scan was positive for tumors known to express VIP receptors.[85] One resulted from recurrence of resected breast cancer (Fig. 9), and the other from a recurrence of neurofibroma in the neck (Fig. 10). These data demonstrate that (a) we can label peptides with ^{99m}Tc efficiently without compromising their receptor specificity and biological activity and (b) target lesions *in vivo* that express specific receptors. Most importantly, benign breast atypia were not delineated, suggesting an absence of false positives, while malignant recurrences not identified by current methods were clearly identified, overcoming the problem of false negatives. These positive results support

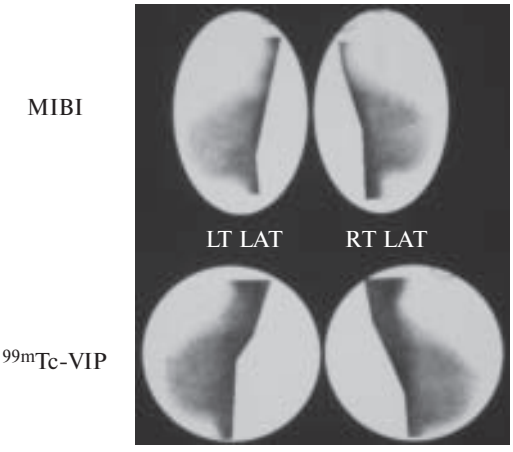

Fig. 8. A 47-year-old female with suspicious mammogram had normal SestaMIBI scan and normal ^{99m}Tc-VIP scan. Right breast biopsy showed only calcium deposit.

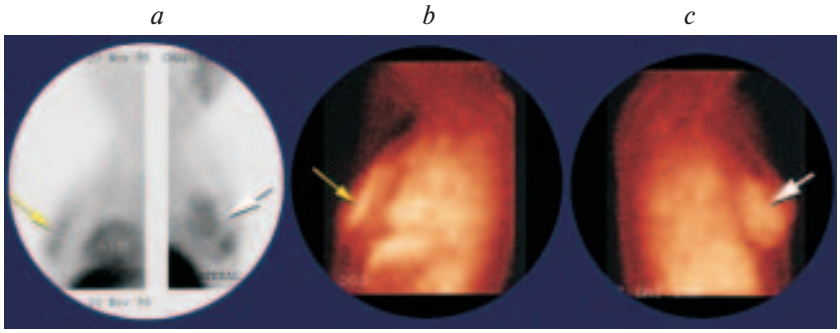

Fig. 9. A 42-year-old woman with prior left mastectomy presented with recurrence in right breast and left operative site. Lateral images with ^{99m}Tc-SestaMIBI (*a*) show uptake in the chest wall and right breast (arrows). Left-side view (*b*) obtained 15 min after injection of ^{99m}Tc-VIP and right-side view (*c*) obtained 1 h after injection of ^{99m}Tc-VIP show same lesions (arrows) perhaps with better intensity than on corresponding ^{99m}Tc-SestaMIBI (*a*).

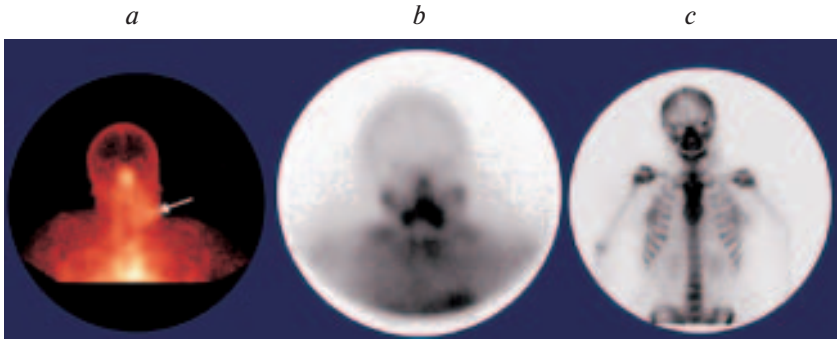

Fig. 10. A 20-year-old woman with a history of neurofibroma of brain in childhood presented with mass in left neck that was evident for 1 month obtained with ^{99m}Tc-VIP scan (*a*), ^{99m}Tc-MIBI scan (*b*), and bone scan (*c*). ^{99m}Tc-MIBI scan (*b*) was negative. Bone scan (*c*) showed faint blood pool. However, ^{99m}Tc-VIP scan (*a*) showed unequivocally positive uptake (arrow). Immunohistology of lesion showed that it was a high-grade spindle cell sarcoma.

the hypothesis that oncogene expression could be imaged *in vivo* with ^{99m}Tc antisense PNAs.

2.2. PNA-peptide probes. PNAs hybridize tightly to RNA, resist nuclease attack, and demonstrate antisense activity *in vitro*.[94] RNA hybridized to uncharged oligonucleotide derivatives, such as PNA, is not recognized by RNase H. Hence, PNA does not catalyze degradation of its bound RNA, but inhibits mRNA translation solely by hybridization arrest, and thus provides an opportunity for diagnostic application. Antisense activity in cells, however, requires microinjection of PNAs into nuclei. This stems from poor cellular uptake,[95] which was ten times less efficient than uptake of phosphorothioates in a variety of mammalian cells.[96] To alleviate this situation, cellular uptake might be improved by addition of a variety of ligands.[74,97]

2.2.1. Design of PNA-peptide conjugates. The insulin-like growth factor 1/insulin like growth factor 1 receptor (IGF1/IGF1R) system plays a major regulatory role in development, cell cycle progression, and the early phase of tumorigenicity.[98] Small peptides have been designed by molecular modeling as analogs of natural IGF1. Similarly, a phage display experiment revealed breast tumor affinity by the cyclized peptide L-CNGRC.[99] The most effective IGF1 peptide analog, JB3, D-CSKAPKLPAAYC, inhibits growth of certain cancer cell lines and competes with the natural ligand for binding to the IGF1R.[100] The JB3 peptide has two Cys residues, one at each terminus, which are disulfide linked to form a loop with limited flexibility, favoring a conformation for binding to the receptor. The use of D-amino acids gave the peptide stability against cellular proteases. A reverse sequence was synthesized with respect to the normal L-amino acid sequence to account for the reversal of chirality.

Thus, we hypothesized that conjugation of the D-peptide analog with an antisense PNA against an effective target sequence of IGF1R mRNA[100] would provide cell-type specificity and increase cellular uptake by those cells overexpressing IGF1R. To reduce the complexity of the synthesis, a smaller version of JB3, called JB9, D-CSKC, was selected for conjugation with the PNA (see Fig. 3, *B*). Cellular uptake of the PNA-peptide conjugate, a control with two D-Ala residues in the peptide in place of D-Ser-Lys, and a control PNA without a peptide adduct, were studied in murine BALB/c3T3 cells, which express low levels of murine IGF1R, in p6 cells, which are BALB/c3T3 cells which overexpress a trans-

Table 1. IGF1R antisense and control sequences

PNA-peptides and PNA, composition	Structure of PNA-peptides and PNA
PNAP1 antisense+IGF1 peptide	H—Gly—CCGCTTCCTTTC—CONH—Gly_4—Cys—Ser—Lys—Cys—CO_2H
PNAP2 antisense+control peptide	H—Gly—CCGCTTCCTTTC—CONH—Gly_4—Cys—Ala—Ala—Cys—CO_2H
PNA1 antisense without peptide	H—Gly—CCGCTTCCTTTC—CO_2H

fected human IGF1R gene,[101] and in human Jurkat cells, which do not express IGF1R,[102] as a negative control.

2.2.2. Preparation of PNA-peptide conjugates. Peptide nucleic acid (PNA), in particular, has shown tremendous potential as an antisense agent.[103] Although PNAs hybridize very strongly and specifically to RNA and DNA, they are taken up poorly by cells, relative to phosphorothioate oligomers,[96] limiting their potential as nucleic acid binding agents. To improve cellular uptake of the IGF1R antisense sequence PNA1 targeted against IGF1R mRNA codons 706—709 [104] (Table 1), it was conjugated to a D-amino acid analog of insulin-like growth factor 1 (IGF1). This analog binds selectively to the cell surface receptor for insulin-like growth factor 1 (IGF1R), which is overexpressed in malignant cells.[101]

The IGF1 D-peptide analog was assembled on (4-methylbenzhydryl)amine (MBHA) resin, then the PNA was extended as a continuation of the peptide. Denaturing SDS gel electrophoresis (Fig. 11) and MALDI-TOF mass

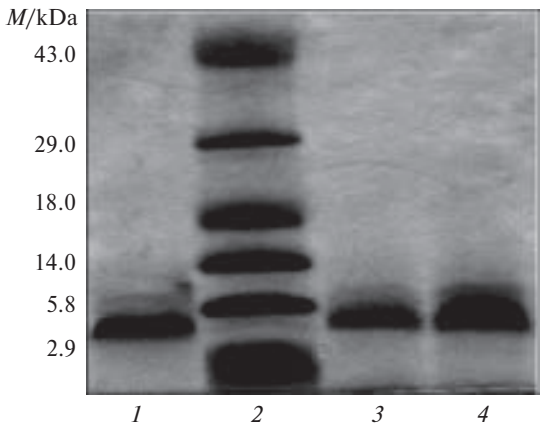

Fig. 11. SDS-PAGE of the PNA-peptide conjugate PNAP1, stained with Coomassie brilliant blue: 0.5 nmol PNAP1 (lane *1*), molecular weight markers (lane *2*), 0.75 nmol PNAP1 (lane *3*), and 1.5 nmol PNAP1 (3.85 kDa) (lane *4*), which migrates between the 5.8 kDa and the 2.9 kDa markers.

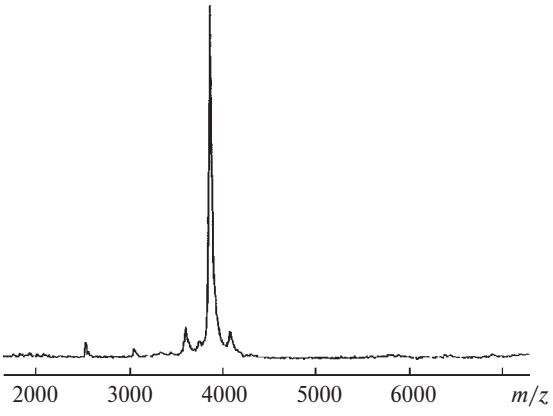

Fig. 12. MALDI-TOF mass spectrum of PNA-peptide conjugate PNAP1 desorbed from a sinapinic acid matrix. The spectrum is an average of eight pulses. Experimental mass 3854.5 Da; calculated mass 3850.7 Da.

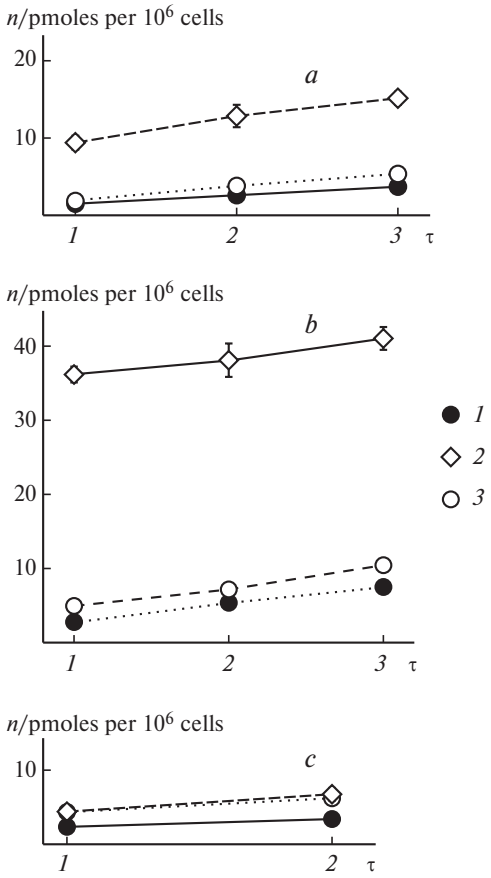

Fig. 13. Cellular uptake of radiolabeled PNA and PNA-peptides by mammalian cells incubated with 1 μ*M* [^{14}C]PNA1 (*1*), [^{14}C]PNAP1 (*2*), and [^{14}C]PNAP2 (*3*) at 37 °C.[74] Data are presented in terms of pmoles oligonucleotide per 10^6 cells Balb/c3T3 (*a*), p6 (*b*), and Jurkat (*c*). Each data point in *a* and *b* represents the mean ±SEM of three replicates. Each data point in *c* represents the mean ± variance of two replicates.

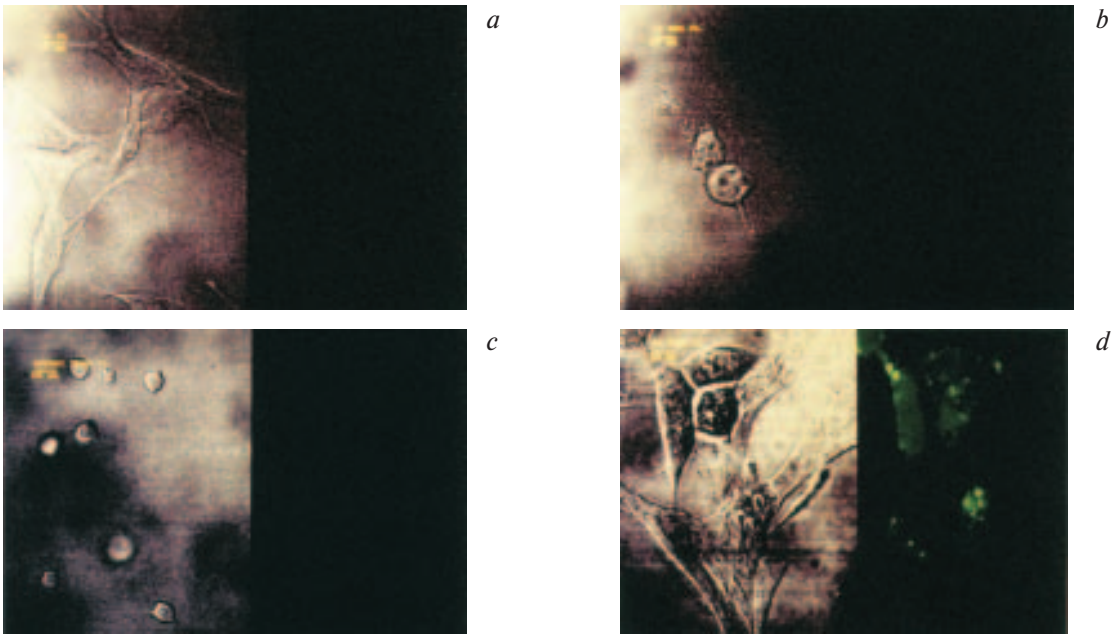

Fig. 14. Confocal microscopy of mammalian cells incubated with 1 μ*M* fluorescein derivatives for 4 h at 37 °C. Left: phase contrast. Right: fluorescence. p6 Cells incubated with fluorescein along (*a*), p6 cells incubated with fluoresceinated PNA1 (*b*), p6 cells incubated with fluoresceinated PNAP1 peptide conjugate (*c*), and Jurkat cells incubated with fluoresceinated PNAP1 peptide conjugate (*d*).

spectrometry (Fig. 12) were consistent with the chimeric sequence.

2.2.3. PNA-peptide binding to cells. The conjugate and control sequences can be radiolabeled with ^{14}C or fluorescently labeled with fluorescein isothiocyanate.[74] Cellular uptake of the PNA-peptide conjugate PNAP1, the control PNAP2 with two alanines in the peptide, and a control PNA1 without the peptide segment, were studied in three cell lines: murine BALB/c3T3 cells, which express low levels of murine IGF1R; p6 cells, which are BALB/c3T3 cells overexpressing a transfected human IGF1R gene; human Jurkat cells, which do not express IGF1R, as a negative control. The specific PNAP1 conjugate displayed much higher uptake than the control PNA1, but only in cells expressing IGF1R, measured with both the ^{14}C-conjugate (Fig. 13) and the fluoresceinyl-conjugate (Fig. 14).[74]

This approach may allow cell-specific application of PNAs as gene expression diagnostics *in vivo*. In addition to the cyclized IGF1 D-peptide analog D-CSKC, we will test a D-peptide analog of L-CNGRC, which revealed breast tumor affinity in a phage display experiment.[99] In prostate cancer cells, for comparison, addition of dihydrotestosterone or a nuclear localization peptide to a c-*MYC* antisense PNA permitted some nuclear localization and Myc reduction in LNCaP cells expressing androgen receptor after 24-h exposure to 10 m*M* PNA.[105] It would appear that use of a peptide analog specific for a cell surface receptor is far more effective than a steroid capable of binding to a cytoplasmic protein after unassisted uptake.

3. Direction of further studies

3.1. Preparation of ^{99m}Tc-PNA-peptides antisense to cyclin D1, *ERBB2*, c-*MYC*, and p53 mRNAs and specific for IGF1 or NGR receptors

3.1.1. Design of chelator-PNA-peptides. The oncogene-specific chelator-PNA-peptide conjugates will be assembled by solid phase synthesis,[74] beginning from the C-terminus. First the IGF1 D-peptide analog D-CSKC or NGR D-peptide analog D-CRGNC will be extended from (4-methylbenzhydryl)amine (MBHA) resin, followed by a Gly_4 spacer, using Fmoc coupling. Control peptides with three Ala replacements in the center, D-CAAAC, will also be prepared.

Because PNA hybridization is so strong and specific, oligomers as short as 12 residues (Table 2) will be extended by Fmoc coupling from the N-termini of the peptides. Experience to date with PNAs argues for targeting the initiation codon, using sequences that overlap with those phosphorothioates that we or others have used successfully as antisense probes. It should be noted that while PNA hybridizes strongly with DNA and RNA at physiological salt concentrations,[74,103] invasion of double helical DNA by a PNA single strand, which is not a target of this proposal, is slow at intranuclear ionic strength.[106] For critical analysis of sequence dependence, control sequences will include 4 central mismatches to preclude antisense hybridization.

The hybrid PNA-peptides will be further modified to permit efficient radiolabeling with ^{99m}Tc by extending a

Table 2. Antisense and mismatch PNA sequences for cyclin D1, *ERBB2*, c-*MYC*, and p53 mRNAs

Target and characteristics	Sequence	Features of structure
cyclin D1 antisense	5′-CTGGTGTTCCAT	codons 1 to 4
cyclin D1 mismatch	5′-CTGG**ACAA**CCAT	4 central mismatches
ERBB2 antisense	5′-CATGGTGCTCAC	codons −3 to 1
ERBB2 mismatch	5′-CATG**CACT**TCAC	4 central mismatches
c-*MYC* antisense	5′-GCATCGTCGCGG	codons −3 to 1
c-*MYC* mismatch	5′-GCAT**GTCT**GCGG	4 central mismatches
p53 antisense	5′-CCCCCTGGCTCC	exon 10
p53 mismatch	5′-CCCC**TACC**CTCC	4 central mismatches

five amino acid chelator from the N-terminus of the PNA, Aba-Gly^2-D-Ala^3-Gly^4-Gly^5 (GAGG) using Fmoc coupling. A similar strategy was pursued earlier to prepare a ^{99m}Tc-DNA-peptide.[107]

3.1.2. Synthesis and purification of chelator-PNA-peptides. The desired chelator-PNA-peptide conjugates will be synthesized, purified, and characterized as described in Section 2. Recent observations (Section 2),[74] except that automated Fmoc coupling of PNA monomers will be carried out on our PE Biosystems 8909 synthesizer, which has the capability and programs to execute this assembly, and has successfully produced c-*MYC* antisense PNA-peptides for NIH CA42960. The conjugates will normally be purified by reversed phase liquid chromatography at 50 °C. Homogeneity will be analyzed by electrophoresis on SDS-PAGE gels[74] and by capillary electrophoresis on open capillaries under peptide conditions. Molecular masses will be determined by electrospray or MALDI-TOF mass spectrometry.[74] The criterion for adequate purity in our experiments will be 95%.

3.1.3. Labeling of chelator-PNA-peptides with ^{99m}Tc. Purified chelator-PNA-peptide conjugates will be labeled with ^{99m}Tc in high specific activity. The radiolabeling method will be similar to that with the peptide labeling.*

* Briefly, to accurately weighed 10 mg chelator-PNA-peptide 600 μL of 0.05 *M* Na_3PO_4 solution, pH 12, will be added, followed by the addition of 75 mg $SnCl_2 \cdot 2H_2O$ in 15 μL of 0.05 *M* HCl and 20—25 μCi freshly eluted $^{99m}TcO_4^-$ in 200 μL saline. The mixture will be incubated for 15 min at 90 °C, cooled to 22 °C, and pH will be adjusted to ~7 by the addition of 1 mL of 0.05 *M* NaH_2PO_4 solution at pH 4.6. The resultant reaction mixture will be examined for free ^{99m}Tc using reversed phase C_{18} microbond HPLC (Rainin, Emeryville, CA) coupled to a UV detector, NaI (Tl) radioactivity monitor, and a rate meter. Mobile phase will consist of 0.1% trifluoroacetic acid in water (solvent A) and 0.1% trifluoroacetic acid in acetonitrile (solvent B). The gradient will be adjusted to distinctly separate ^{99m}Tc free and bound to the PNA. Colloid formation, if any, will be determined using instant thin layer chromatography (ITLC-SG, Gelman Sciences, Ann Arbor, MI) using pyridine/acetic acid/water (3 : 5 : 1.5) as a solvent. Our experience indicates that using this system we obtain high labeling efficiency, usually >95%. Colloid formation is less than 3%.

3.2. Specificity of uptake and mRNA hybridization of ^{99m}Tc-PNA-peptides in normal and transformed human breast cancer cell lines in culture

3.2.1. Tumor cell lines. The human breast cancer cell line BT474, isolated from the pleural effusion of an invasive ductal carcinoma, overexpresses c-*MYC* and *ERBB2* oncogenes.[108] A selected subline produces aggressive solid tumors following several passages through mice.[109] Our diagnostic approaches will be examined in this doubly positive cell line, which Dr. Gail Colbern kindly sent to us, compared with the doubly negative control breast tumor line MDA-MB-435 (American Type Culture Collection, Rockville, MD), which does not overexpress either oncogene.[6] The lines will be maintained in log phase at 37 °C in DMEM supplemented with 2 *mM* glutamine, 5000 U · mL^{-1} pen/strep, and 10% fetal bovine serum (Sigma Chemical Co., St. Louis, MO)

3.2.2. Quantitation of cyclin D1, *ERBB2*, c-*MYC*, and p53 mRNAs by QRT-PCR. After growing the cell lines to 70—80% confluence, parallel cell cultures treated for 24 h at 37 °C with 100 *nM* unlabeled chelator-PNA-peptide will be lysed and total RNA will be isolated. The RNA will be reverse-transcribed using 50 μg · mL^{-1} oligo (dT), 500 μ*M* deoxynucleotide triphosphate, and 200 units of Superscript II reverse transcriptase (Life Technologies) for 1 h at 37 °C, and the resulting first strand cDNA diluted and used as template for QRT-PCR analysis.

Oncogene mRNAs will be quantitated by utilizing the 5′ nuclease activity of Taq DNA polymerase to generate a real-time quantitative DNA analysis assay.[110] A non-extendible oligonucleotide hybridization probe with 5′-fluorescent and 3′-rhodamine (quench) moieties is present during the extension phase of the PCR. Degradation and release of the fluorescent moiety due to the 5′ nuclease activity results in peak emission at 518 nm. The increase in fluorescence is monitored during the complete amplification process (real-time). The expression of the housekeeping gene, cyclophilin 33A, and the nuclear transcription factor binding protein (TBP) will be used to normalize for variances in input cDNA. Published primer and fluorescent probes sets will be used to

measure cyclin D1,[111] *ERBB2*,[112] c-*MYC*,[113] and p53 [114] mRNAs.

3.2.3. Quantitation of cyclin D1, *ERBB2*, c-*MYC*, and p53 antigens by Western blotting. After growing the cell lines to 70—80% confluence, parallel cell cultures treated for 24 h at 37 °C with 100 *nM* unlabeled chelator-PNA-peptide will be lysed, the cell debris will be pelleted, 100 mg total protein will be extracted from each sample, separated electrophoretically under reducing conditions on a discontinuous 12% polyacrylamide gel, and transferred to a PVDF membrane. After transfer, membranes will be blocked with 5% nonfat dry milk and probed with mouse monoclonal antibodies (Santa Cruz Biotechnology, Santa Cruz, CA) against cyclin D1, ErbB2, c-Myc, and p53 followed by a horseradish peroxidase-conjugated goat anti-mouse immunoglobulin G (IgG) (Jackson ImmunoResearch, West Grove, PA) and Super Signal luminescent substrate (Pierce Chemicals, Rockford, IL), as we have done previously.[10,14,35]

3.2.4. ^{99m}Tc-PNA-peptide internalization by tumor cells. BT474 and MDA-MB-435 cells at 70—80% confluence will be treated with 1, 10, and 100 *nM* ^{99m}Tc-PNA-peptide specific and control probes in culture medium including serum and incubated at 37 °C. At 15 min, 30 min, and 1, 2, 4, 8, 16, and 24 h later, cells will be washed twice with PBS, then the dishes will be imaged using a STARCAM (GE, Milwaukee, WI) gamma camera equipped with a parallel hole collimator. To follow the time course of uptake, all images will be recoreded for one hour. Alternatively, labeled cells will be lysed with a biomaterial fluor cocktail and counted in a liquid scintillation spectrometer.[96] This experiment will reveal the time of greatest signal:background ratio, the time of greatest concentration of specifically bound probe relative to unbound probe. That time will depend on the rate of uptake, rate of cellular trafficking, rate of specific hybridization to target mRNA, rate of mRNA degradation, rate of new mRNA transcription, and rate of probe efflux from cells. The rate of PNA probe dissociation from specific targets will be negligible in this time frame, compared to other phenomena.

3.2.5. ^{99m}Tc-PNA-peptide subcellular localization. The above experiment will reveal the time of greatest signal/background, the time of greatest concentration of specifically bound probe relative to unbound probe. At that time point, treated cell samples will be lysed gently for subcellular fractionation by differential centrifugation.[96,115] The resulting fractions will be dissolved in a biomaterial fluor cocktail and counted in a liquid scintillation spectrometer. Previous investigations with radiolabeled oligonucleotide derivatives, including PNAs, all showed significant nuclear concentration.[96]

3.2.6. ^{99m}Tc-PNA-peptide S1 nuclease protection of target mRNAs. To test the hypothesis that specific PNA probes will bind their intended targets, RNA will be extracted from treated cells as in Section 3.2.2, then hydrolyzed with nuclease S1 [12] to destroy all single-stranded RNA not protected by ^{99m}Tc-PNA-peptide PNA probe. Aliquots of each hydrolysis reaction will be electrophoresed on native, non-denaturing 20% polyacrylamide gels in TBE, then imaged with X-ray film or the PhosphorImager to identify double-stranded complexes of ^{99m}Tc-PNA-peptide with RNA fragments. The virtually uncharged PNA probes will not enter the gel under these conditions, unless hybridized to unlabeled RNA fragments. This test is not as stringent as unlabeled PNA binding to labeled RNA target. However, the use of antisense and mismatch control probes and positive and negative cell lines should provide a clear answer to the question of specificity. Electrophoretic standards will include a single-stranded [^{33}P]RNA ladder and a single ^{99m}Tc-PNA-peptide hybridized to its specific RNA dodecamer target. The time of maximum duplex band intensity might be the ideal time for imaging of whole animals, assuming that PNA hybridization to its RNA targets is slower than tissue distribution and tumor permeation. *In vivo* experiments presented in Section 3.3 below will answer that question directly.

3.3. Specificity and sensitivity of scintigraphic imaging of ^{99m}Tc-PNA-peptides bound to cyclin D1, *ERBB2*, c-*MYC*, and p53 mRNAs in human breast cancer xenografts in nude mice

3.3.1. Tumor xenografts. Animals will be cared for in an AAALAC-approved institutional animal care facility. In groups of 5 subjects, 6—8 week old female Balb/c nu/nu mice, we will implant $1 \cdot 10^6$ BT474 or MDA-MB-435 cells subcutaneously by sterile 25 gauge needle into the flank of each subject. The subcutaneous site yields a localized, measureable, recoverable tumor. Analgesics will be supplied, in case of pain or distress from tumor cell implantation, in the form of a tylenol-codeine elixir mixed 3 mL to 250 mL H_2O and be given *ad libitum* in the drinking water. The subjects will be given sterile mouse chow and water *ad libitum* and maintained in standard microisolator cages. In the overall experimental design, groups bearing BT474 cells and groups bearing MDA-MB-435 cells will be administered antisense and mismatch ^{99m}Tc-PNA sequences targeted against cyclin D1, *ERBB2*, c-*MYC*, and p53 mRNAs (Table 2), with IGF1, NGR, or Ala_3 D-peptide analogs, yielding a total of 2 cell lines × 3 peptides × 8 PNAs × 5 subjects = 240 subjects. Each pair of oncogene PNAs will be tested separately to allow experiments of manageable scale, running over at least two years. The number of subjects per group was set at five based on the hypothesis of a strong positive for oncogene overexpression of ~100 copies per cell, or a strong negative for normal oncogene expression of ~1 per cell, as explained below.

3.3.2. Rationale for mRNA detection with ^{99m}Tc-PNA-peptides. Mice bearing subcutaneous tumor xenografts approximately 0.5 cm (~1 g) in diameter after about one week of growth will be administered approximately 1 μCi ^{99m}Tc-PNA-peptide through a lateral tail vein with a sterile 25 gauge needle, then imaged using a GE (Milwaukee, WI) STARCAM gamma camera coupled to a parallel hole collimator. Pharmacokinetic studies have typically found that about 2% (20 μCi) of labeled oligonucleotide or peptide distributes to a 0.5 cm (~1 g) tumor in a mouse within an hour. PNA-peptides are actively taken up into tumor cells against a concentration gradient.[74]

A one-gram tumor consists of approximately 10^9 cells. Assuming each tumor cell carries ~100 copies of a particular oncogene mRNA when overexpressed, there will be approximately 10^{11} probe binding sites per cell. Even if only 20% of these sites are hybridized with ^{99m}Tc-PNA-peptide molecules and only one ^{99m}Tc-PNA-peptide is bound to each oncogene mRNA, there will be approximately $2 \cdot 10^{10}$ ^{99m}Tc atoms immobilized in the tumor. Each μCi of ^{99m}Tc has $1.15 \cdot 10^9$ atoms. Therefore, ~$2 \cdot 10^{10}$ atoms will be equivalent to ~18 μCi ^{99m}Tc in a gram of tumor. This calculated quantity of radioactivity is comparable to the amount of label likely to distribute to the tumor, and will readily permit delineation of a tumor in a mouse, or, for that matter, in a human. In the negative case of normal oncogene expression, we expect only ~1 mRNA copy per cell, generating no more than 1% of the signal to be seen in the positive case.

Maximum signal-to-noise will occur when most of the RNA bound to labeled PNA is still intact, but most unbound labeled PNA has effluxed from cells and been excreted. That time point is predicted to occur within 12 h of administration, but must be determined experimentally through serial observations of subjects over 24 h after administration. Our goal for signal:background ratio is 10; that would provide a comfortable margin for diagnostic applications.

3.3.3. ^{99m}Tc-PNA-peptide administration and metabolism. Five normal Balb/c nude mice will be injected through a lateral tail vein with approximately 100 μCi of ^{99m}Tc-PNA-peptide and placed in metabolic cages. Urine will be collected for up to 4 h, filtered through a 0.22 μm filter for removal of particulate matter and analyzed by HPLC using the analytical conditions identical to those of the quality control method. Elution of radioactivity at any other retention time than that of the ^{99m}Tc-PNA will indicate if the agent has metabolically degraded and was unstable *in vivo*.

3.3.4. ^{99m}Tc-PNA-peptide imaging and tissue distribution studies. These studies will be carried out in nude mice bearing human breast tumors approximately 1 cm or less in diameter. A pre-determined quantity of ^{99m}Tc bound to a corresponding chelator-PNA-peptide will be administered to groups of five mice each through a lateral tail vein. At 15 min, 30 min, and 1, 2, 4, 8, 16, and 24 h post-injection mice will be lightly anesthetized, imaged using a STARCAM (GE, Milwaukee, WI) gamma camera equipped with a parallel hole collimator. For images, 300 000 counts will be recorded on a paper plate. Mice will then be euthanized in a halothane gas chamber and tissues will be dissected. These will be washed free of any blood, blotted free of liquid, weighed, and radioactivity associated with each tissue will be counted in a Packard (5000 series) automatic gamma counter, together with a standard radioactive solution of a known quantity prepared at the time of injection. Results will be expressed as percent of injected dose per gram of tissue (% ID g^{-1}). Data will be evaluated statistically using Student´s test.

3.3.5. ^{99m}Tc-PNA-peptide internalization and subcellular localization in tumor cells. Tumor samples will also be disrupted to single cell suspensions, washed, then lysed with a biomaterial fluor cocktail and counted in a liquid scintillation spectrometer.[96] This will determine whether or not tumor cells in a tumor behave similarly to those in cell culture.

Single cell suspensions will be lysed gently for subcellular fractionation by differential centrifugation.[96,115] The resulting fractions will be dissolved in a biomaterial fluor cocktail and counted in a liquid scintillation spectrometer. Again, we will compare the cellular trafficking pattern of probes in a tumor with probes in cultured cells.

3.3.6. ^{99m}Tc-PNA-peptide S1 nuclease protection of target mRNAs. To test the hypothesis that specific PNA probes will bind their intended targets, RNA will be extracted from excised tumor cells as in 3.2.2 above, then hydrolyzed with nuclease S1 and analyzed electrophoretically as in Section 3.2.6. This experiment will answer the question of probe interactions with mRNAs in tumors vs. cultured cells.

3.3.7. Correlative measurements of oncogene mRNA expression. Tumor xenografts will also be implanted in animals not given ^{99m}Tc-labeled probes. Parallel tumors removed at the same time as gamma imaging will be analyzed by QRT-PCR as in Section 3.2.2 to determine mRNA levels in BT474 tumors *vs*. MDA-MB-435 tumors. Thus, we will obtain a direct comparison of tumor imaging results with tumor mRNA levels.

3.4. Specificity of uptake and mRNA hybridization of ^{99m}Tc-PNA-peptides in organotypic cultures of freshly excised normal and cancerous human breast cells

3.4.1. Isolation of fibroblasts and epithelial cells. To attain the goal of 10 clear examples of organotypic cultures of breast cancer cells probed with ^{99m}Tc antisense

PNA, up to 30 patient samples will be collected and processed. After approval from our Institutional Review Board and informed consent from the patient, a breast specimen will be transported to the laboratory immediately after removal. Fibroblasts will be isolated by placing the specimen in DMEM/10% FCS and allowing them to grow outward onto 100 mm diameter dishes. For epithelial cells, a trypsin digestion of the specimen will be performed and the suspension grown in Mammary Epithelial Cell Media (Clonetics, San Diego, CA).

3.4.2. Three-dimensional reconstruction of cellular layers in organotypic culture. Two mixtures will be prepared on ice, one with and the other without cells. The acellular mixture contains DMEM in 10% fetal bovine serum with rat tail collagen, pH adjusted to 7.4 with NaOH. The cellular mixture contains fibroblasts in DMEM in 10% FCS with rat tail collagen, adjusted to pH 7.4. The acellular mixture will be added at room temperature in 12 mm dishes. After this has hardened, the cellular mixture will be heated to 37 °C and placed over the acellular material. The culture will be incubated at 37 °C in 5% CO_2 and fed twice weekly with DMEM in 10% FCS. Ten days after plating the fibroblasts, a layer of Matrigel (Becton Dickinson, Bedford, MA) will be added, and allowed to harden; then, mammary epithelial cells in DMEM containing 5% serum, estrogen, progesterone, prolactin, hydrocortisone, cholera toxin, insulin, EGF, and transferrin will be placed over the Matrigel. The reconstruct will be fed with the DMEM/5% FCS and growth factors for 4, 8, or 12 days prior to fixation, sectioning and staining with hematoxylin and eosin.

3.4.3. ^{99m}Tc-PNA-peptide internalization by tumor cells. After establishment of the organotypic cultures of each tumor sample, ^{99m}Tc-PNA-peptides will be added to the culture medium, and the plates will be incubated for the optimal time, at the optimal probe concentrations, as described in Section 3.3.5. Specificity of uptake as a function of probe sequence will be examined. S1 nuclease protection of RNA target sequences provides the most critical test for desired probe localization, and will be carried out as described in Section 3.3.6.

4. Conclusion

We propose to detect the onset of activated oncogene expression during the earliest stages of breast cancer, when surgical intervention could significantly reduce mortality. No method is currently available to measure levels of specific mRNAs *in vivo*.

To solve this problem, we hypothesize that ^{99m}Tc-PNA-peptides will be taken up by human breast cancer cells, hybridize to complementary mRNA targets, permit scintigraphic imaging of oncogene mRNAs in human breast cancer xenografts in a mouse model, and ultimately allow imaging of oncogene mRNAs in human tissue prior to any other outward indication of disease. Peptide nucleic acids (PNAs) display superior ruggedness and hybridization properties as a diagnostic tool for gene expression, but they are not readily taken up by normal or malignant cells. However, we have observed that certain ^{99m}Tc-peptides can delineate tumors, that PNA-peptides designed to bind to IGF1 receptors on malignant cells are taken up specifically and concentrated in nuclei, and that ^{99m}Tc can be chelated to PNA-peptides designed to bind to IGF1 receptors.

We are preparing ^{99m}Tc-PNA-peptides capable of binding to the receptor for IGF1, with complementary PNA sequences that hybridize specifically to mRNAs for overexpressed cyclin D1, *ERBB2*, and c-*MYC* oncogenes, and for mutant tumor suppressor p53. Antisense PNA 12-mer probes have been synthesized for those targets. One of the PNA probes has been prepared with an N-terminal peptide chelating moiety, and successfully labeled with ^{99m}Tc, as well as a chelator-ligand control. Preparations of chelator peptide-PNA-ligand peptides are underway, together with their application in organotypic cultures. We will test the specificity of uptake and mRNA hybridization of our ^{99m}Tc-PNA-peptide probes in normal human epithelial cells *vs*. transformed human breast cancer cells.

If these initial experiments show promise, we will administer ^{99m}Tc-PNA-peptide probes to cohorts of nude mice bearing human breast cancer xenografts and determine the sensitivity and specificity of scintigraphic imaging of the targeted oncogene mRNAs in the tumors, relative to the nonspecific signals expected in the liver, gall bladder, and kidneys. We will compare the imaging results to real time QRT-PCR measurements of those mRNAs in tumor cells removed from the subjects and to the same mRNAs in liver, gallbladder and kidneys. These experiments will test our concept for noninvasive detection of gene expression in living cells and tissues.

Unequivocal, specific images, if obtained, will provide a proof-of-principle for noninvasive detection of oncogene expression in early-stage breast cancer cells. If the animal trials are encouraging, similar probes will be tested in normal and cancerous mammary tissue specimens from volunteer subjects. Such a scintigraphic imaging technique should be applicable to any particular gene of interest in a cell or tissue type with characteristic receptors.

This work was financially supported by the US DOE grant BER ER63055 and US NIH grant CA42960 to E. W.

References

1. M. Namavari, J. R. Barrio, T. Toyokuni, S. S. Gambhir, S. R. Cherry, H. R. Herschman, M. E. Phelps, and Satyamurthy, *Nucl. Med. Biol.*, 2000, **27**, 157.

2. R. Hustinx, C. Y. Shiue, H. Zhuang, D. McDonald, M. Lanuti, E. Lambright, J. G. Smith, J. S. Karp, P. Lu, S. L. Eck, and A. A. Alavi, *J. Nucl. Med.*, 2000, **41**, 264.
3. V. Ponomarev, M. Dubrovin, J. Balatoni, R. Finn, R. G. Blasberg, and J. G. Tjuvajev, *J. Nucl. Med.*, 2000, **41**, 263.
4. R. T. Greenlee, T. Murray, S. Bolden, and P. A. Wingo, *CA Cancer J. Clin.*, 2000, **50**, 7.
5. C. J. Baines, in *Fundamental Problems in Breast Cancer*, Eds. H. G. Paterson and A. W. Lees, Marcus Nijhoff: Boston, 1987, 25.
6. K. J. Martin, B. M. Kritzman, L. M. Price, B. Koh, C. P. Kwan, X. Zhang, A. Mackay, M. J. O´Hare, C. M. Kaelin, G. L. Mutter, A. B. Pardee, and R. Sager, *Cancer Res.*, 2000, **60**, 2232.
7. J. M. Bishop, *Cell*, 1991, **64**, 235.
8. E. R. Sauter, M. Herlyn, S. C. Liu, S. Litwin, and J. A. Ridge, *Clin. Cancer Res.*, 2000, **6**, 654.
9. J. P. Vaughn, J. D. Iglehart, S. Demirdji, P. Davis, L. E. Babiss, M. H. Caruthers, and J. R. Marks, *Proc. Natl. Acad. Sci. USA*, 1995, **92**, 8338.
10. E. Wickstrom and F. L. Tyson, in *Oligonucleotides as Therapeutic Agents*, D. Chadwick and G. Cardew, Wiley: London, 1997, **209**, 124; discussion 137.
11. E. L. Wickstrom, T. A. Bacon, A. Gonzalez, D. L. Freeman, G. H. Lyman, and E. Wickstrom, *Proc. Natl. Acad. Sci. USA*, 1988, **85**, 1028.
12. E. Wickstrom, T. A. Bacon, and E. L. Wickstrom, *Cancer Res.*, 1992, **52**, 6741.
13. Y. Huang, R. Snyder, M. Kligshteyn, and E. Wickstrom, *Molecular Medicine*, 1995, **1**, 647.
14. J. B. Smith and E. Wickstrom, *J. Natl. Cancer Inst.*, 1998, **90**, 1146.
15. M. R. Bishop, J. D. Jackson, S. R. Tarantolo, B. O´Kane-Murphy, P. L. Iversen, E. Bayever, S. M. Joshi, J. G. Sharp, J. L. Pierson, P. I. Warkentin, J. O. Armitage, and A. Kessinger, *J. Hematotherapy*, 1997, **6**, 441.
16. E. Bayever, K. M. Haines, P. L. Iversen, R. W. Ruddon, S. J. Pirruccello, C. P. Mountjoy, M. A. Arneson, and L. J. Smith, *Leukemia Lymphoma*, 1994, **12**, 223.
17. P. W. Hinds, S. F. Dowdy, E. N. Eaton, A. Arnold, and R. A. Weinberg, *Proc. Natl. Acad. Sci. USA*, 1994, **91**, 709.
18. J. Bartkova, J. Lukas, H. Muller, M. Strauss, B. Gusterson, and J. Bartek, *Cancer Res.*, 1995, **55**, 949.
19. J. Adelaide, G. Monges, C. Derderian, J. F. Seitz, D. Birnbaum, *Br. J. Cancer*, 1995, **71**, 64.
20. K. Helin and E. Harlow, *Trends Cell Biol.*, 1992, **3**, 43.
21. D. W. Goodrich and W.-H. Lee, *Biochim. Biophys. Acta*, 1993, **1155**, 43.
22. J. R. Nevins, *Science*, 1992, **258**, 424.
23. C. Deng, P. Zhang, J. W. Harper, S. J. Elledge, and P. Leder, *Cell*, 1995, **82**, 675.
24. H. D. Matsushime, E. Quelle, S. A. Shurtleff, M. Shibuya, C. J. Sherr, and J.-Y. Kato, *Mol. Cell Biol.*, 1994, **14**, 2066.
25. A. Arnold, H. G. Kim, R. D. Gaz, R. L. Eddy, Y. Fukushima, M. G. Byers, T. B. Shows, and H. M. Kronenberg, *J. Clin. Invest.*, 1989, **83**, 2034.
26. T. Motokura and A. Arnold, *Genes Chromosomes Cancer*, 1993, **7**, 89.
27. W. Jiang, S. M. Kahn, P. Zhou, Y. J. Zhang, A. M. Cacace, A. S. Infante, S. Doi, R. M. Santella, I. B. Weinstein, *Oncogene*, 1993, **8**, 3447.
28. D. E. Quelle, R. A. Ashmun, S. A. Shurtleff, J. Y. Kato, D. Bar-Sagi, M. F. Roussel, and C. J. Sherr, *Genes Dev.*, 1993, **7**, 1559.
29. H. Lovec, A. Sewing, F. C. Lucibello, R. Muller, and T. Moroy, *Oncogene*, 1994, **9**, 323.
30. M. S. Rieber and M. Rieber, *Biochem. Biophys. Res. Commun.*, 1995, **216**, 422.
31. C. B. Vos, N. T. Ter Haar, J. L. Peterse, C. J. Cornelisse, and M. J. van de Vijver, *J. Pathol.*, 1999, **187**, 279.
32. P. Collecchi, A. Passoni, M. Rocchetta, E. Gnesi, E. Baldini, and G. Bevilacqua, *Int. J. Cancer*, 1999, **84**, 139.
33. T. Utsumi, N. Yoshimura, M. Maruta, S. Takeuchi, J. Ando, Y. Mizoguchi, and N. Harada, *Int. J. Cancer*, 2000, **89**, 39.
34. F. S. Kenny, R. Hui, E. A. Musgrove, J. M. Gee, R. W. Blamey, R. I. Nicholson, R. L. Sutherland, and J. F. Robertson, *Clin. Cancer Res.*, 1999, **5**, 2069
35. E. R. Sauter, M. Nesbit, S. Litwin, A. J. Klein-Szanto, S. Cheffetz, and M. Herlyn, *Cancer Res.*, 1999, **59**, 4876.
36. D. J. Slamon, G. M. Clark, S. G. Wong, W. J. Levin, A. Ullrich, and W. L. McGuire, *Science*, 1987, **235**, 177.
37. M. J. van de Vijver, J. L. Peterse, W. J. Mooi, P. Wisman, J. Lomans, O. Dalesio, and R. Nusse, *N. Engl. J. Med.*, 1988, **319**, 1239.
38. A. Stark, B. S. Hulka, S. Joens, D. Novotny, A. D. Thor, L. E. Wold, M. J. Schell, L. J. Melton, 3rd, E. T. Liu, and K. Conway, *J. Clin. Oncol.*, 2000, **18**, 267.
39. R. Goldman, R. B. Levy, E. Peles, and Y. Yarden, *Biochemistry.*, 1990, **29**, 11024.
40. A. L. Schechter, M. C. Hung, L. Vaidyanathan, R. A. Weinberg, T. L. Yang-Feng, U. Francke, A. Ullrich, and L. Coussens, *Science*, 1985, **229**, 976.
41. M. H. Kraus, W. Issing, T. Miki, N. C. Popescu, and S. A. Aaronson, *Proc. Natl. Acad. Sci. USA*, 1989, **86**, 9193.
42. M. Alimandi, A. Romano, M. C. Curia, R. Muraro, P. Fedi, S. A. Aaronson, P. P. Di Fiore, and M. H. Kraus, *Oncogene*, 1995, **10**, 1813.
43. Y. Kokai, J. A. Cohen, J. A. Drebin, and M. I. Greene, *Proc. Natl. Acad. Sci. USA*, 1987, **84**, 8498.
44. M. F. Press, M. C. Pike, V. R. Chazin, G. Hung, J. A. Udove, M. Markowicz, J. Danyluk, W. Godolphin, M. Sliwkowski, and R. Akita, *Cancer Res.*, 1993, **53**, 4960.
45. J. S. Ross and J. A. Fletcher, *Oncologist*, 1998, **3**, 237.
46. M. A. Cobleigh, C. L. Vogel, and N. J. Tripathy, *Proc. Am. Soc. Clin. Oncol.*, 1998, **17**, 97.
47. D. Slamon, B. Leyland-Jones, and S. Shak, *Proc. Am. Soc. Clin. Oncol.*, 1998, **17**, 98.
48. J. Bertram, M. Killian, W. Brysch, K. Schlingensiepen, and M. Kneba, *Biochem. Biophys. Res. Commun.*, 1994, **200**, 661.
49. J. P. Vaughn, J. Stekler, S. Demirdji, J. K. Mills, M. H. Caruthers, J. D. Iglehart, and J. R. Marks, *Nucleic Acids Res.*, 1996, **24**, 4558.
50. K. F. Pirollo, Z. Hao, A. Rait, C. W. Ho, and E. H. Chang, *Biochem. Biophys. Res. Commun.*, 1997, **230**, 196.
51. E. M. Berns, J. G. Klijn, W. L. van Putten, I. L. van Staveren, H. Portengen, and J. A. Foekens, *Cancer Res.*, 1992, **52**, 1107.

52. E. M. Blackwood and R. N. Eisenman, *Science*, 1991, **251**, 1211.
53. K. H. Moberg, T. J. Logan, W. A. Tyndall, and D. J. Hall, *Oncogene*, 1992, **7**, 411.
54. K. H. Moberg, W. A. Tyndall, and D. J. Hall, *J. Cell Biochem.*, 1992, **49**, 208.
55. E. Wickstrom, *Prospects for Antisense Nucleic Acid Therapy of Cancer and AIDS*, Wiley-Liss, New York, 1991.
56. J. B. Smith and E. Wickstrom, *Methods Enzymol.*, 2000, **314**, 537.
57. P. H. Watson, R. T. Pon, and R. P. Shiu, *Cancer Res.*, 1991, **51**, 3996.
58. L. Meng, L. Lin, H. Zhang, M. Nassiri, A. R. Morales, and M. Nadji, *Mutat. Res.*, 1999, **435**, 263.
59. A. D. Thor, D. H. Moore, II, S. M. Edgerton, E. S. Kawasaki, E. Reihsaus, H. T. Lynch, J. N. Marcus, L. Schwartz, L. C. Chen, and B. H. Mayall, *J. Natl. Cancer Inst.*, 1992, **84**, 845.
60. A. D. Thor, D. A. Berry, D. R. Budman, H. B. Muss, T. Kute, I. C. Henderson, M. Barcos, C. Cirrincione, S. Edgerton, C. Allred, L. Norton, and E. T. Liu, *J. Natl. Cancer Inst.*, 1998, **90**, 1346.
61. Z. Tong, G. Singh, and A. J. Rainbow, *Photochem. Photobiol.*, 2000, **71**, 201.
62. M. Gurnani, P. Lipari, J. Dell, B. Shi, and L. L. Nielsen, *Cancer Chemother. Pharmacol.*, 1999, **44**, 143.
63. J. Nemunaitis, S. G. Swisher, T. Timmons, D. Connors, M. Mack, L. Doerksen, D. Weill, J. Wait, D. D. Lawrence, B. L. Kemp, F. Fossella, B. S. Glisson, W. K. Hong, F. R. Khuri, J. M. Kurie, J. J. Lee, J. S. Lee, D. M. Nguyen, J. C. Nesbitt, R. Perez-Soler, K. M. Pisters, J. B. Putnam, W. R. Richli, D. M. Shin, G. L. Walsh, and J. Merritt, *J. Clin. Oncol.*, 2000, **18**, 609.
64. W. C. Broaddus, Y. Liu, L. L. Steele, G. T. Gillies, P. S. Lin, W. G. Loudon, K. Valerie, R K. Schmidt-Ullrich, and H. L. Fillmore, *J. Neurosurg.*, 1999, **91**, 997.
65. L. Xu, K. F. Pirollo, W. H. Tang, A. Rait, and E. H. Chang, *Hum. Gene Ther.*, 1999, **10**, 2941.
66. A. M. Belikova, V. F. Zarytova, and N. I. Grineva, *Tetrahedron Lett.*, 1967, **37**, 3557.
67. P. C. Zamecnik and M. L. Stephenson, *Proc. Natl. Acad. Sci. USA*, 1978, **75**, 280.
68. S. Agrawal, *Antisense Therapeutics*, Humana Press, Totowa NJ, 1996.
69. E. Wickstrom, *Clinical Trials of Genetic Therapy with Antisense DNA and DNA Vectors*, Marcel Dekker, New York, 1998.
70. P. T. Ho, K. Ishiguro, E. Wickstrom, and A. C. Sartorelli, *Antisense Research and Development*, 1991, **1**, 329.
71. S. Agrawal, *Trends in Biotechnology*, 1996, **14**, 376.
72. B. P. Monia, E. A. Lesnik, C. Gonzalez, W. F. Lima, D. McGee, C. J. Guinosso, A. M. Kawasaki, P. D. Cook, and S. M. Freier, *J. Biol. Chem.*, 1993, **268**, 14514.
73. S. Agrawal, Z. Jiang, Q. Zhao, D. Shaw, Q. Cai, A. Roskey, L. Channavajjala, C. Saxinger, and R. Zhang, *Proc. Natl. Acad. Sci. USA*, 1997, **94**, 2620.
74. S. Basu and E. Wickstrom, *Bioconjugate Chem.*, 1997, **8**, 481.
75. T. M. Tan, B. W. Kalisch, J. H. van de Sande, R. C. Ting, and Y. H. Tan, *Antisense Nucleic Acid Drug Dev.*, 1998, **8**, 95.
76. J. M. Aramini and M. W. Germann, *Biochem. Cell Biol.*, 1998, **76**, 403.
77. V. K. Rait and B. R. Shaw, *Antisense Nucleic Acid Drug Dev.*, 1999, **9**, 53.
78. B. R. Shaw, D. Sergueev, K. He, K. Porter, J. Summers, Z. Sergueeva, and V. Rait, *Methods Enzymol.*, 2000, **313**, 226.
79. S. Basu and E. Wickstrom, *Tetrahedron Lett.*, 1995, **36**, 4943.
80. J. Hughes, A. Astriab, H. Yoo, S. Alahari, E. Liang, D. Sergueev, B. R. Shaw, and R. L. Juliano, *Methods Enzymol.*, 2000, **313**, 342.
81. C. Marwick, *JAMA*, 1998, **280**, 871.
82. R. Y. Walder and J. A. Walder, *Proc. Natl. Acad. Sci. USA*, 1988, **85**, 5011.
83. M. A. Stalteri and S. J. Mather, *Nucl. Med. Commun.*, 2000, **21**, 374.
84. M. L. Thakur, V. R. Pallela, P. M. Consigny, P. S. Rao, D. Vessileva-Belnikolovska, and R. Shi, *J. Nucl. Med.*, 2000, **41**, 161.
85. M. L. Thakur, C. S. Marcus, S. Saeed, V. Pallela, C. Minami, L. Diggles, H. Le Pham, R. Ahdoot, and E. A. Kalinowski, *J. Nucl. Med.*, 2000, **41**, 107.
86. P. S. Rao, M. L. Thakur, V. Pallela, R. Patti, K. Reddy, H. Li, S. Sharma, H. L. Pham, L. Diggles, C. Minami, and C. S. Marcus, *Nucl. Med. Biol.*, 2001, **28**, 445.
87. P. S. Rao, V. R. Pallela, D. Vassileva-Belnikolovska, D. Jungkind, and M. L. Thakur, *Nucl. Med. Commun.*, 2000, **21**, 1063.
88. M. Eisenhut and U. Haberkorn, *Eur. J. Nucl. Med.*, 2000, **27**, 1589.
89. W. Mier, R. Eritja, A. Mohammed, U. Haberkorn, and M. Eisenhut, *Bioconjugate Chem.*, 2000, **11**, 855.
90. W. Mier, R. Eritja, A. Mohammed, U. Haberkorn, and M. Eisenhut, *J. Labelled Comp. Radiopharm.*, 2001, **42**, 115.
91. V. R. Pallela, M. L. Thakur, S. Chakder, and S. Rattan, *J. Nucl. Med.*, 1999, **40**, 352.
92. V. R. Pallela, M. L. Thakur, P. M. Consigny, P. S. Rao, D. Vasileva-Belnikolavska, and R. Shi, *Thromb. Res.*, 1999, **93**, 191.
93. J. C. Reubi, *J. Nucl. Med.*, 1995, **36**, 1825.
94. J. C. Hanvey, N. J. Peffer, J. E Bisi, S. A. Thomson, R. Cadilla, J. A. Josey, D. J. Ricca, C. F. Hassman, M. A. Bonham, and K. G. Au, *Science*, 1992, **258**, 1481.
95. M. A. Bonham, S. Brown, A. L. Boyd, P. H. Brown, D. A. Bruckenstein, J. C. Hanvey, S. A. Thomson, A. Pipe, F. Hassman, and J. E. Bisi, *Nucleic Acids Res.*, 1995, **23**, 1197.
96. G. D. Gray, S. Basu, and E. Wickstrom, *Biochem. Pharmacol.*, 1997, **53**, 1465.
97. L. Good and P. E. Nielsen, *Proc. Natl. Acad. Sci. USA*, 1998, **95**, 2073.
98. R. Baserga, *Cancer Res.*, 1995, **55**, 249.
99. W. Arap, R. Pasqualini, and E. Ruoslahti, *Science*, 1998, **279**, 377.
100. Z. Pietrzkowski, D. Wernicke, P. Porcu, B. A. Jameson, and R. Baserga, *Cancer Res.*, 1992, **52**, 6447.
101. Z. Pietrzkowski, C. Sell, R. Lammers, A. Ullrich, and R. Baserga, *Mol. Cell Biol.*, 1992, **12**, 3883.

102. R. B. Lal, D. L. Rudolph, T. M. Folks, and W. C. Hooper, *Leuk. Res.*, 1993, **17**, 31.
103. M. Egholm, O. Buchardt, L. Christensen, C. Behrens, S. M. Freier, D. A. Driver, R. H. Berg, S. K. Kim, B. Norden, and P. E. Nielsen, *Nature*, 1993, **365**, 566.
104. A. Ullrich, A. Gray, A. W. Tam, T. Yang-Feng, M. Tsubokawa, C. Collins, W. Henzel, T. Le Bon, S. Kathuria, and E. Chen, *EMBO J.*, 1986, **5**, 2503.
105. L. C. Boffa, S. Scarfi, M. R. Mariani, G. Damonte, V. G. Allfrey, U. Benatti, and P. L. Morris, *Cancer Res.*, 2000, **60**, 2258.
106. L. Good and P. E. Nielsen, *Antisense Nucleic Acid Drug Dev.*, 1997, **7**, 431.
107. S. Basu, H. R. Kolan, M. L. Thakur, and E. Wickstrom, *J. Labeled Comp. Radiopharm.*, 1995, **37**, 350.
108. X. Le Roy, C. Escot, J. P. Brouillet, C. Theillet, T. Maudelonde, J. Simony-Lafontaine, H. Pujol, and H. Rochefort, *Oncogene*, 1991, **6**, 431.
109. H. J. van Slooten, B. A. Bonsing, A. J. Hiller, G. T. Colbern, J. H. van Dierendonck, C. J. Cornelisse, and H. S. Smith, *Br. J. Cancer*, 1995, **72**, 22.
110. P. M. Holland, R. D. Abramson, R. Watson, and D. H. Gelfand, *Proc. Natl. Acad. Sci. USA*, 1991, **88**, 7276.
111. M. M. Kennedy, S. Biddolph, S. B. Lucas, D. D. Howells, S. Picton, J. O. McGee, I. Silva, V. Uhlmann, K. Luttich, and J. J. O´Leary, *J. Clin. Pathol.*, 1999, **52**, 569.
112. I. Bièche, P. Onody, I. Laurendeau, M. Olivi, D. Vidaud, R. Lidereau, and M. Vidaud, *Clin. Chem.*, 1999, **45**, 1148.
113. I. Bièche, I. Laurendeau, S. Tozlu, M. Olivi, D. Vidaud, R. Lidereau, and M. Vidaud, *Cancer Res.*, 1999, **59**, 2759.
114. I. Arany, A. Yen, and S. K. Tyring, *Anticancer Res.*, 1997, **17**, 1281.
115. Y. Daaka and E. Wickstrom, *Oncogene Res.*, 1990, **5**, 267.

Received September 25, 2001